

MRI segmentation using Fuzzy C-means and radial basis function neural networks

A. H. Rasooli¹, M. Ashtiyani², P. M. Birgani¹, S. Amiri¹, P. Mirmohammadi² and M. R. Deevband^{2,*}

¹Department of Medical Physics and Biomedical Engineering, Tehran University of Medical Sciences, Iran

²Department of Biomedical Engineering and Medical Physics, Faculty of Medicine, Shahid Beheshti University of Medical Sciences, Tehran, Iran

Image segmentation is one of the major preprocessing steps of magnetic resonance imaging (MRI) analysis in many medical and research applications. Accurate differentiation between three major soft tissues of the brain – grey matter, white matter and cerebrospinal fluid – is a key step in structural and functional brain analysis, visualization of the brain’s anatomical structures and measurement, diagnosis of neuro-degenerative disorders and image-guided interventions as well as surgical planning. We propose a new methodological approach in segmentation of MRI images of the brain structure. Although various methods for MRI segmentation have been proposed, improvement of soft, automatic and precise MRI segmentation methods are worth a try. The proposed method has almost the same results as those from recent efforts in this field. However, it performs better in the presence of noise and RF-filed inhomogeneity.

Keywords: Fuzzy C-means, magnetic resonance imaging, neural networks, segmentation, radial basis function.

MAGNETIC resonance imaging (MRI) as a non-invasive tool offers a wealth of information for medical examination. Many clinical and research applications using MR images require a precise segmentation of biological tissues based on their different grey level intensities¹. So in MRI processing, image segmentation plays a crucial role in defining the desired tissues in terms of their spatial location, size and shape, as well as establishing and improving therapeutic projects by means of evaluating the therapeutic effect. Moreover, it is also the basis of 3D visualization and reconstruction^{2,3}. Although manual segmentation of images is a time-consuming process and susceptible to human errors, MRI segmentation has been previously performed manually by trained radiologists; there are many recent advanced methods which have been employed to segment MRI⁴. However, there is still a lack of automatic MRI analysis method which results in precise delineation of tumours and is reproducible in reliable segmentation of images. Furthermore, lack of clearly defined edges induces large inter- and intra-observer

variability, which downgrades the significance of the analysis of the resulting segmentation, thus calling for automatic segmentation methods^{2,5,6}. A variety of methods have been used to segment medical images including MRI⁷. Usually, segmentation is one of the most time-consuming pre-processing steps. Hence, automatic algorithms with fast responses are utilized in most non-surgical and clinical applications. For example, threshold-based method is used for segmentation of liver vessels in CT and MRI images as a fast automatic algorithm⁸. By contrast, in some research applications, atlas-based algorithms are used to differentiate exactly the soft tissues from each other⁹. Since they need registration of images in atlas space, these methods are too time consuming to be used in clinics. Moreover, they need expert knowledge in building the atlas and choosing the appropriate one⁷. Artificial neural network (ANN), as a computational or mathematical model inspired by biological nervous systems, is widely used for image segmentation in different applications^{10,11}. In these methods an ANN is trained with a dataset and is expected to perform segmentation on a new, unknown dataset¹².

Intelligent fuzzy classifiers are another important group of methods which are applied on medical images for segmentation purposes. These soft tissue classification methods deal better with unwanted artifacts, e.g. partial volume effect or noisy images. Most popularly, Fuzzy C-means (FCM) is a data clustering method, wherein a grade is used to define the membership degree of each data point to a cluster. This technique was originally advocated in 1981 by Jim Bezdek as an improvement over earlier clustering methods^{13,14}. It provides a method which shows how to group data points that populate some multidimensional space into a specific number of different clusters. In 2008, Birgani *et al.*¹ used FCM algorithm combined with a competitive neural network to find prototypes of the MRI histogram. In their approach, competitive neural network specifies the centre of clusters regarding each tissue type and FCM performs soft clustering. Their study was inspired by the method that Mehta *et al.*¹⁵ used in their study.

Radial basis function (RBF) network is a kind of artificial neural network which uses Gaussian as activation function. The network output is a linear combination of

*For correspondence. (e-mail: mdeevband@sbmu.ac.ir)

neuron parameters and radial basis functions of the inputs. Radial basis function networks have many uses, including system control, classification, time series prediction and function approximation¹⁶.

Inspired by the recent work, in this study, the RBF network with gradient descent learning algorithm is employed to perform function approximation and find independent prototypes of histograms pertaining to main types of brain tissue. Then, FCM is employed to perform classification. Hence, the main objective of this study is to provide a new approach to segment brain images based on histogram prototype detection. Based on our previous work, we have hypothesized that RBF networks can perform segmentation with better precision and lower calculation cost. This way, segmentation of the whole brain MRI images can be performed fast, with acceptable precision.

Methods

For this study, simulated MRI image data sets were downloaded from the brain website¹⁷. Also, one clinical data acquired from a cerebral palsy (CP) patient was used to show the clinical applicability of this algorithm on real data. All analyses were done using Matlab R2013a software (Mathworks Inc., Natick, MA, USA). Also NNtool package of Matlab was used for design, generation and training of the RBF neural network.

Histogram modelling and prototypes

Distribution of the numerical data is represented by a graphical tool called histogram¹⁸⁻²⁰. Image histogram acts as a graphical representation of grey level distribution in a digital image. As mentioned before, the main objective of this study is to find the independent components of the histogram, which are related to different tissues. In order to differentiate between brain tissue types, the histogram of each image was calculated, and the peaks which were related to each independent tissue with respect to noise level were selected. For segmentation purpose, we had to differentiate between independent peaks and separate them to specific prototypes regarding different tissues. For this purpose, using an RBF neural network, we tried to fit an exact Gaussian on each prototype and separate the related tissue type from other parts.

Radial basis function neural network

Radial basis function neural network (RBF NN) is a family of artificial neural networks that uses a nonlinear function called radial basis function as an activation function. The architecture of an RBF network is shown in Figure 1. Vector x is used as an input to all radial basis functions,

each with different parameters. In these networks, neurons work specifically and the output is a combination of inputs passed through nonlinear activation functions of neurons²¹. These networks are presented as a three-layer feed forward structure: the first layer called input layer works as a distributor of inputs to the next layer. The second layer called hidden layer contains neurons with nonlinear activation function. As Gaussian functions are frequently used in this layer, we chose this network for our Gaussian fitting application.

$$\phi_i(x) = \phi(\|x - \mu_i\|; \sigma_i) = e^{-\left(\frac{\|x - \mu_i\|^2}{2\sigma_i^2}\right)}, \tag{1}$$

in which ϕ_i is the output of the i th hidden neuron in the second layer with centre μ_i and σ_i spread²². Finally, the output layer is just a linear combination (weighted sum) of the hidden layer outputs:

$$y(x_i) = \sum_{j=1; k} w_j \phi(\|x_i - c_j\|) + w_0. \tag{2}$$

This output is the estimation of histogram and the basis functions of the hidden layer neurons are independent prototypes regarding each tissue type.

To simulate the stated RBF neural networks, algorithms were implemented in Matlab programming environment (MATLAB and Statistics Toolbox Release 2013b). To determine the appropriate architecture for RBF neural network, networks with different architectures (different number of hidden neurons) were created. By training these networks, we were able to find the network structure with best accuracy. The RBF networks need not be trained with different network structures, since appropriate architecture could be obtained spontaneously in the learning process, by adding a neuron to the network's hidden layer at iteration of training.

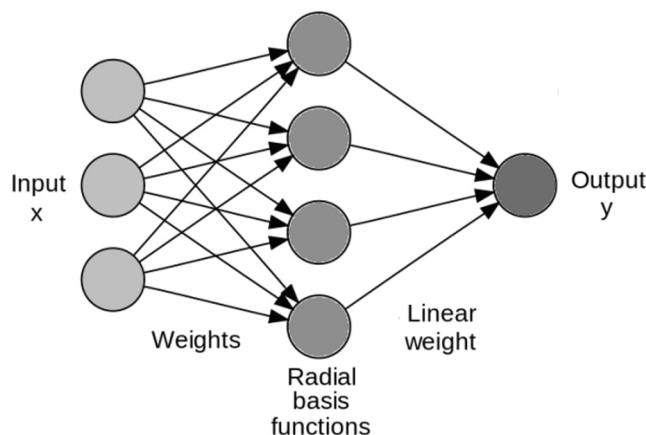


Figure 1. Schematic of RBF network.

Optimizing model parameters

This network is made up of a linear combination of Gaussian basis functions; therefore we need to use an optimization algorithm that minimizes the variance accounted for (VAF) cost function between estimated and main histogram of the image. VAF is a cost function based on the least mean square error criteria and defined as

$$\text{VAF} = \left(1 - \frac{O-D}{O}\right) \times 100, \quad (3)$$

where O is the output of the RBF network and D is the desired value of the histogram. For the best estimation we need to maximize this VAF value to near 1 and find our desired Gaussian basis functions.

Hence we need to optimize three parameters for each neuron and one parameter for the network. Three main parameters of the Gaussian basis functions include: centre (μ_i), spread (σ_i) and effective amplitude (weight) of each neuron which must be optimized using gradient descent algorithm.

Gradient descent is one of the most common algorithms to perform optimization and by far the most widely accepted method to optimize neural networks. Considering all of parameters in the network, gradient descent optimization method calculates the gradient of a loss function and then is fed to the optimization method, which in turn uses it to update the parameters, in an attempt to minimize the loss function. The steps are as follows: (1) All weights should be initialized to random values. It is preferred to start from small values. (2) Inputs which are histogram counts will be provided to the neural network to compute the output and its comparison to target. (3) Each parameter w_{ij} will be updated using, $w_{ij(t+1)} = w_{ij(t)} + \mu \delta_j y_j$. (4) Steps 2 and 3 will be repeated until the error is less than the specified value.

This way the parameters of each Gaussian (hidden neuron) will be optimized to make the best estimation.

Also, as mentioned before, we need to optimize the number of hidden neurons to an optimum level that estimates all the main peaks with acceptable precision, while number of peaks as prototypes is chosen automatically and objectively.

The best way to find the optimum number of hidden neurons is by trial and error. Regarding this, by changing the number of these neurons, we found the best answer for this parameter, where our cost function met our predefined error condition.

Classification

After training the network, the basis functions of the hidden neurons (Gaussian functions) are responsible for

representation of the different brain tissue types containing: white matter (WM), grey matter (GM), Cerebrospinal fluid (CSF) and possible tumours. Also, due to the noise level and partial volume effect, there may be some pixels that are not completely related to one of the tissue types. Hence, using Fuzzy C-means algorithm²³, it is possible to set a membership function for each pixel to show its membership in each tissue type and apply a soft segmentation.

Results

As mentioned before, we trained RBF network using gradient descent algorithm. In each training procedure, this network converged after 40 iterations and the error rate satisfied a predefined level before increasing the error rate (Figure 2). Also, to find the optimum number of hidden neurons, we trained the network with different number of hidden neurons.

This algorithm was applied to all the images in the mentioned dataset. In other words, it was applied to both noise-free images and to entirely noisy images with RF inhomogeneity. After finding the appropriate number of hidden neurons, the resulting Gaussian functions were fitted appropriately and the prototypes regarding different main tissue types were found precisely (Figure 3). Also,

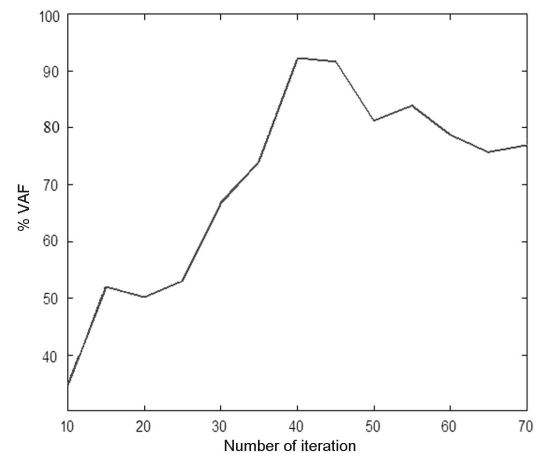


Figure 2. Percentage of variance accounted for per epoch.

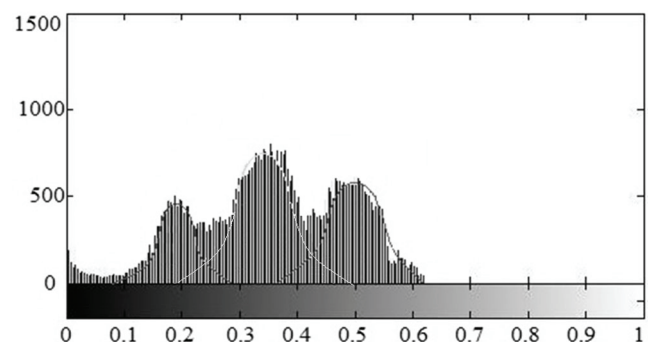


Figure 3. Performance of the RBF network in finding the histogram prototypes in one of the noisiest images.

Table 1. Results of new segmentation algorithm compared to our previous method

		Dice			Jaccard			Average sensitivity	Average specificity	Average precession
		GM	WM	CSF	GM	WM	CSF			
Present method	Noise = 0% RF inhomogeneity = 0%	89.1	86.9	72.4	84.3	73.4	62.3	92.4	92.2	95.3
	Noise = 3% RF inhomogeneity = 20%	83.6	80.0	66.5	74.8	69.7	54.9	88.7	87.1	91.2
	Noise = 7% RF inhomogeneity = 40%	80.1	75.3	58.4	72.2	65.6	50.1	87.9	85.3	87.3
Our previous method ¹²	Noise = 0% RF inhomogeneity = 0%	82.8	79.0	67.4	80.7	68.4	53.7	Not analysed	Not analysed	Not analysed
	Noise = 3% RF inhomogeneity = 20%	76.4	72.8	57.9	71.6	68.4	49.4	Not analysed	Not analysed	Not analysed
	Noise = 7%	72.9	69.9	49.8	67.8	61.8	41.9	Not analysed	Not analysed	Not analysed
	RF inhomogeneity = 40%							Not analysed	Not analysed	Not analysed

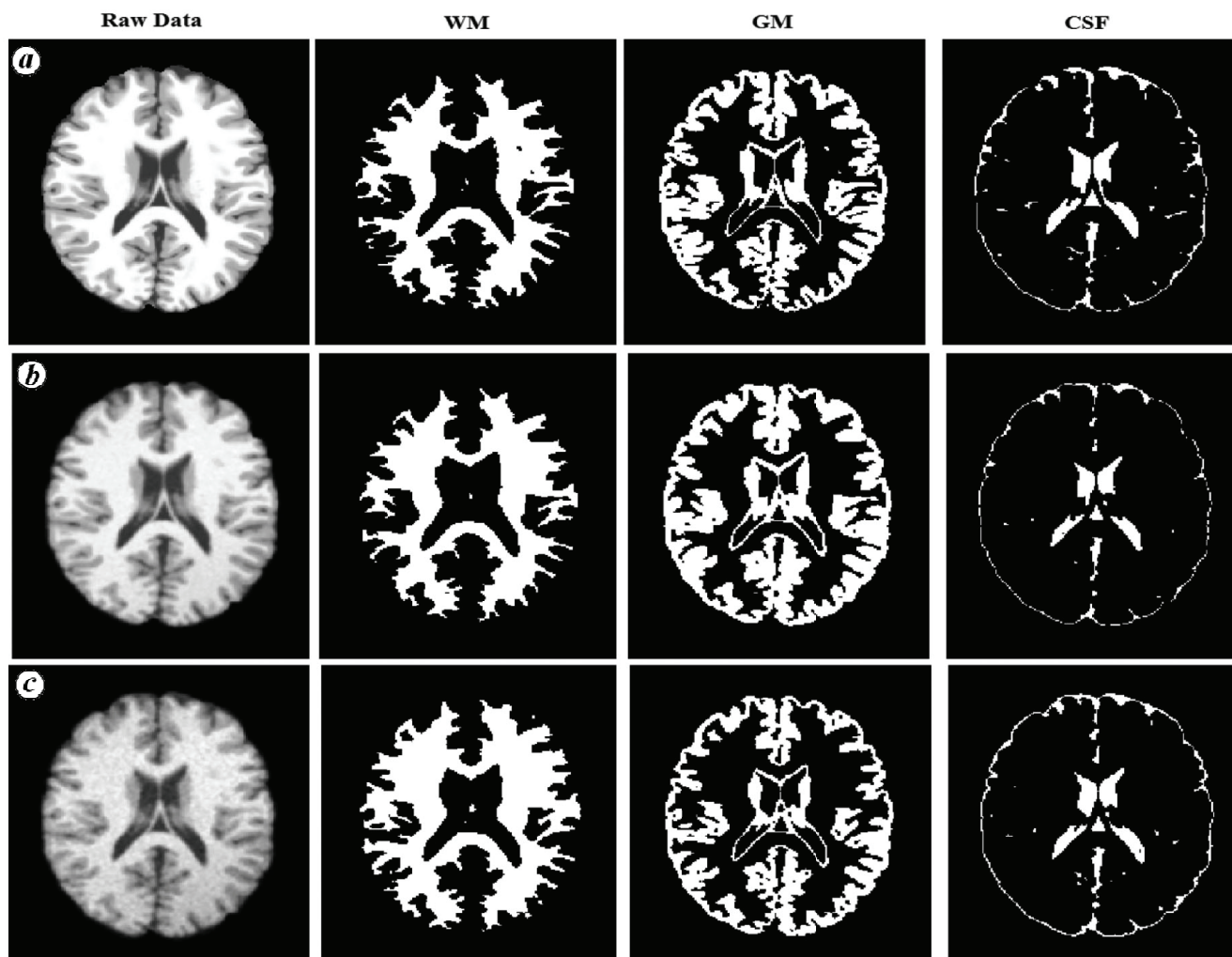


Figure 4. Segmentation of brain web simulation data. *a*, %0 noise and %0 RF inhomogeneity; *b*, %3 noise and %20 RF inhomogeneity; *c*, Image with %7 noise and %40 RF inhomogeneity.

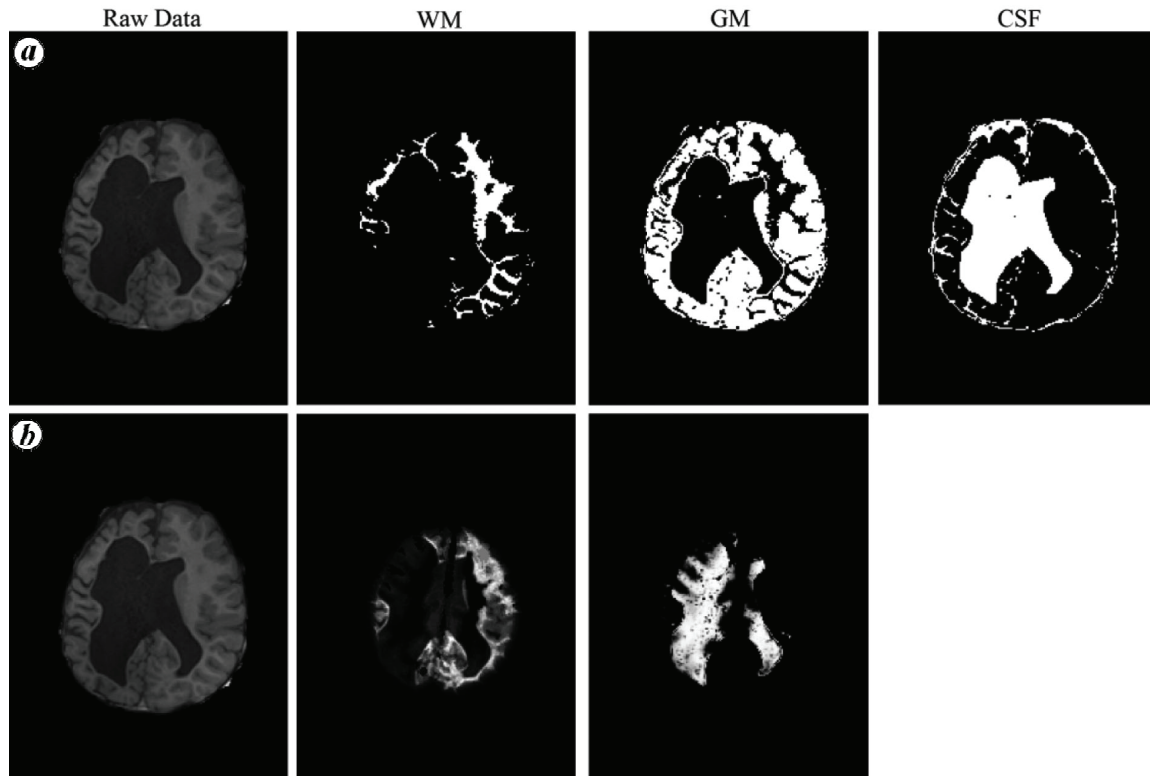


Figure 5. Segmentation of real clinical data. *a*, Segmented with the proposed method; *b*, Segmented with SPM.

the result of applying it on the mentioned dataset is shown in Figure 4.

To evaluate the performance of the proposed segmentation algorithm, a standard and objective method is needed. The performance of the segmentation capability of this algorithm is evaluated using several objective indices. In order to evaluate our proposed algorithm, we used accuracy, sensitivity, specificity and precision which are defined as

$$\text{Sensitivity} = \frac{TP}{(TP + FN)}, \quad \text{Specificity} = \frac{TN}{(TN + FP)},$$

$$\text{Precision} = \frac{TP}{(TP + FP)}, \quad \text{Accuracy} = \frac{TP + TN}{(TP + FP + FN + TN)},$$

where FN, FP, TN and TP denotes false negative, false positive, true negative and true positive respectively. Also, accuracy of the proposed method was assessed using three commonly used measures: Dice similarity index (DI)²⁴ and Jaccard similarity index (JI)²⁵. The similarity metrics represent an overlap between segmented tissues (A) and corresponding ground truth (G). All similarity measures were calculated using the simulated white matter and grey matter of the brain web as the standard ground truth for our simulated dataset. The results are presented in Table 1.

$$DI\% = \frac{2|A \cap G|}{|A| + |G|} \times 100, \quad JI\% = \frac{|A \cap G|}{|A \cup G|} \times 100.$$

The results of this method indicate a great precision, sensitivity and Dice and Jaccard similarity indices in detecting voxels of the grey matter, white matter and cerebrospinal fluid. It can be seen that even in the noisy images with RF inhomogeneity, this algorithm can be applied and has acceptable results.

Also, in order to show the clinical applicability of this method, the proposed method is applied on a real data sample of a cerebral palsy (CP) patient. In the original image, a vast white matter atrophy can be seen which has caused enlargement in brain ventricles and it is filled with CSF and lesion. As this method is not dependent on predefined templates, it can be seen that a good performance is achieved compared to template based methods. Figure 5 shows that this method is able to segment abnormal brain. Also, it is compared with statistical parametric mapping (SPM) segmentation which is a template based method. It can be seen that SPM fails, as it tries to register the image to template, but lesion in the brain causes major misregistration and leads to segmentation failure.

Discussion

Accurate identification of the three brain tissues, GM, WM and CSF is a vital step in structural and functional

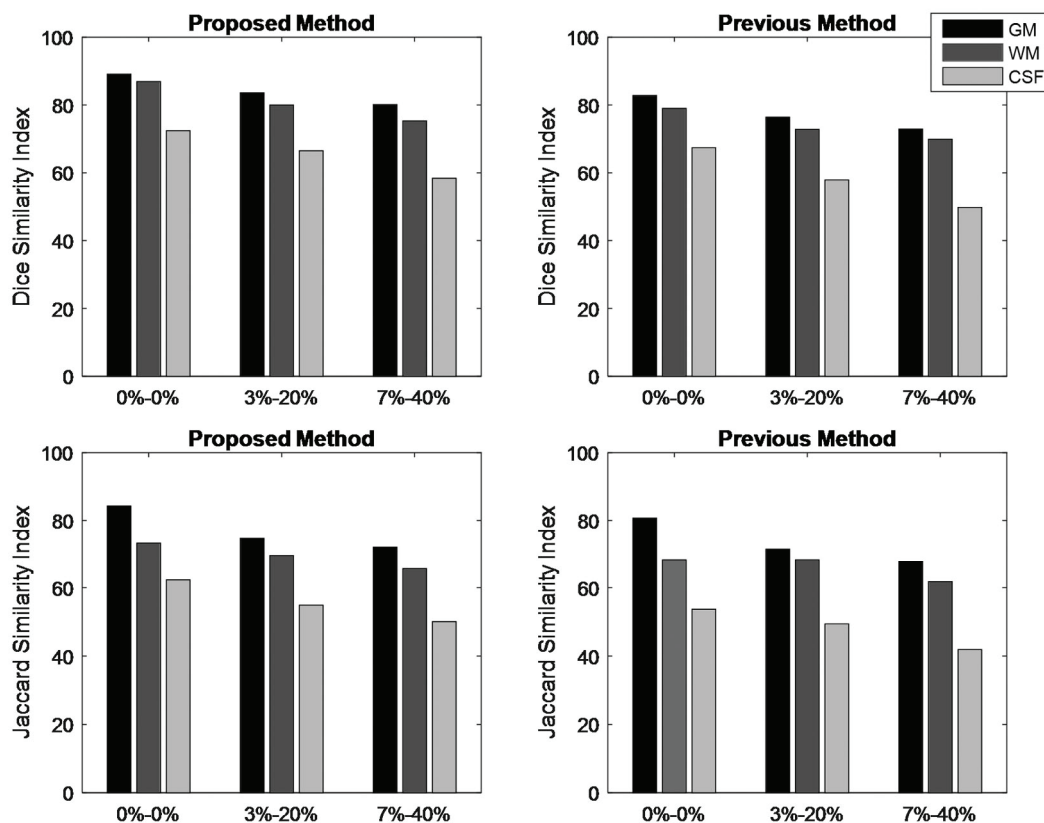


Figure 6. Comparison between proposed method and previous method of tissue segmentation in different noise levels and RF inhomogeneity.

analysis of the brain. Histogram-based algorithms are usually considered as fast, time-consuming and efficient segmentation methods with acceptable precisions. The main challenge in these methods is finding the appropriate peaks and thresholds relating to each type of tissue.

In this paper RBF neural networks for automatic segmentation of MR images have been proposed and its performance evaluated using simulated data. Using this algorithm, the exact and efficient number of tissues is estimated from the histogram, which is further used to segment the tissues using FCM, softly and accurately. Also, this algorithm was applied on real clinical data of CP brain and its performance was compared with a template based segmentation method, which is used for brain analysis applications called SPM. It can be seen that, due to abnormal brain structure and miss-registration, SPM fails to perform an acceptable segmentation. But, in the proposed, intensity-based method, acceptable tissue classification has been possible.

Assessment of the segmented tissues from simulation images, using all of the performance metrics, shows that the proposed method can segment the brain tissues at different noise levels with a high degree of accuracy. Especially, CSF has been segmented more precisely compared to similar studies¹². Figure 6 shows graphically, the

comparison of the newly proposed method with our similar, previously proposed method¹². It can be seen that an improvement in Dice and Jaccard indices are achieved in this method.

Initially, we applied this method only on simulated images to evaluate the performance of our method compared to previous segmentation algorithms. Meanwhile, to show its better performance in clinical applications, the method was applied to a CP brain and the results compared with a template-based method. For further investigation on the performance of this method, it is suggested that the proposed algorithm be applied on real datasets having different noise levels and artifacts, and different lesions and tumours. Furthermore, since this method detects histogram prototypes automatically, it is recommended that its performance be investigated in segmentation of high intensity tumours, which cause specific prototypes.

Conclusion

Segmentation is one of the most crucial steps in brain analysis studies and applications. The proposed method has better performance in different noise levels compared

to similar methods, and it can be developed for scientific and clinical applications. Overall, comparing this method with the existing methods shows that the proposed method has performed better and yielded results with better segmentation, especially in noisy conditions.

Increase in evaluation metrics of the presented RBF-based MR image segmentation system will hopefully help promote more frequent application of MR image segmentation techniques such as measurement of brain's anatomical structures, functional brain analysis, diagnosis of neurodegenerative disorders, image-guided interventions and surgical planning.

1. Birgani, P. M., Ashtiyani, M. and Asadi, S., MRI segmentation using fuzzy *c*-meansclustering algorithm basis neural network. In 3rd International Conference on Information and Communication Technologies: From Theory to Applications, ICTTA 2008, Damascus, Syria, 2008, pp. 1–5.
2. Sun, W. and Wang, Y., Segmentation method of MRI using fuzzy Gaussian basis neuralnetwork. *Neural Inform. Proc.-Lett. Rev.*, 2005, **8**, 19–24.
3. Despotović, I., Goossens, B. and Philips, W., MRI segmentation of the human brain: challenges, methods, and applications. *Comput. Math. Meth. Med.*, 2015, **2015**, 450341(1–23).
4. Mostaar, A. *et al.*, An improved ant colony algorithm optimization for automated MRI segmentation using probabilistic atlas. *Int. J. Innov. Res. Sci. Eng.*, 2015, **3**(12), 399–406.
5. Siyal, M. Y. and Yu, L., An intelligent modified fuzzy *c*-means based algorithm for biasestimation and segmentation of brain MRI. *Pattern Recog. Lett.*, 2005, **26**, 2052–2062.
6. Amiri, S., Movahedi, M. M., Kazemi, K. and Parsaei, H., 3D cerebral MR image segmentationusing multiple-classifier system. *Med. Biol. Eng. Comput.*, 2016, 1–12.
7. Sharma, N. and Aggarwal, L. M., Automated medical image segmentation techniques. *J. Med. Phys./Assoc. Med. Phys. India*, 2010, **35**, 3.
8. Eidheim, O. C., Aurdal, L., Omholt-Jensen, T., Mala, T. and Edwin, B., Segmentation of livervessels as seen in MR and CT images. *Int. Cong. Ser.*, 2004, **1268**, 201–206.
9. Cuadra, M. B., De Craene, M., Duay, V., Macq, B., Pollo, C. and Thiran, J.-P., Dense deformation field estimation for atlas-based segmentation of pathological MR brain images. *Comput. Meth. Prog. Biomed.*, 2006, **84**, 66–75.
10. Chaplot, S., Patnaik, L. and Jagannathan, N., Classification of magnetic resonance brainimages using wavelets as input to support vector machine and neural network. *Biomed. Signal Proc. Control*, 2006, **1**, 86–92.
11. Gletsos, M., Mouggiakakou, S. G., Matsopoulos, G. K., Nikita, K. S., Nikita, A. S. and Kelekis, D., A computer-aided diagnostic system to characterize CT focal liver lesions: design and optimization of a neural network classifier. *IEEE Trans. Informat. Technol. Biomed.*, 2003, **7**, 153–162.
12. Amiri, S., Movahedi, M. M., Kazemi, K. and Parsaei, H., 3D Cerebral MR image segmentation using multiple-classifier system. *Med. Biol. Eng. Comput.*, 2017, **55**, 353–364.
13. Ashtiyani, M., Asadi, S. and Birgani, P. M., ICA-based EEG classification using fuzzy C-mean algorithm. In 3rd International Conference on Information and Communication Technologies: From Theory Applications, ICTTA 2008, Damascus, Syria, 2008, pp. 1–5.
14. Mansoory, M. S., Ashtiyani, M. and Sarabadani, H., Automatic crack detection in eggshell-based on SUSAN edge detector using Fuzzy thresholding. *Mod. Appl. Sci.*, 2011, **5**, 117.
15. Mehta, S. B., Chaudhury, S., Bhattacharyya, A. and Jena, A., A soft-segmentation visualization scheme for magnetic resonance images. *Mag. Reson. Imaging*, 2005, **23**, 817–828.
16. Alvar, A. A., Deevband, M. R. and Ashtiyani, M., Neutron spectrum unfolding using radialbasis function neural networks. *Appl. Radiat. Isot.*, 2017, **129**, 35–41.
17. <http://www.bic.mni.mcgill.ca/brainweb>.
18. Pearson, K., Contributions to the mathematical theory of evolution. *Philos. Trans. R. Soc. London. A*, 1894, **185**, 71–110.
19. Birgani, P. M., Ashtiyani, M., Rasooli, A., Shahrokhnia, M., Shahrokhhi, A. and Mirbagheri, M. M., Can an anti-gravity treadmill improve stability of children with cerebral palsy? The 38th Annual International Conference of the IEE Engineering in Medicine and Biology Society (EMBC), Orlando, USA, 2016, pp. 5465–5468.
20. Ashtiyani, M., Behbahani, S., Asadi, S. and Birgani, P. M., Transmitting encrypted data by wavelet transform and neural network. IEEE International Symposium on Signal Processing and Information Technology, Giza, Egypt, 2007, pp. 385–389.
21. Broomhead, D. S. and Lowe, D., Radial basis functions, multi-variable functional interpolation and adaptive networks. DTIC Document, 1988.
22. Esmaeili, A. and Mozayani, N., Adjusting the parameters of radial basis function networks using particle swarm optimization. In IEEE International Conference on Computational Intelligence for Measurement Systems and Applications, Hong Kong, China, 2009, pp. 179–181.
23. Mirmohammadi, P., Taghavi, A. and Ameri, A., Automatic recognition of acute lymphoblastic leukemia cells from microscopic images. *Int. J. Innov. Res. Sci. Eng.*, 2017, **5**(7), 8–11.
24. Dice, L. R., Measures of the amount of ecologic association between species. *Ecology*, 1945, **26**, 297–302.
25. Jaccard, P., The distribution of the flora in the alpine zone. *New Phytol.*, 1912, **11**, 37–50.

ACKNOWLEDGEMENTS. We acknowledge the Department of Biomedical Engineering and Medical Physics, Tehran University of Medical Sciences and Department of Biomedical Engineering and Medical Physics, Faculty of Medicine, Shahid Beheshti University of Medical Sciences for support.

Received 12 December 2017; revised accepted 12 June 2018

doi: 10.18520/cs/v115/i6/1091-1097